



OPEN

Strain-induced photoconductivity in thin films of Co doped amorphous carbon

SUBJECT AREAS:

SEMICONDUCTORS

GLASSES

ELECTRONIC PROPERTIES AND
MATERIALS

Y. C. Jiang & J. Gao

Department of Physics, The University of Hong Kong, Pokfulam Road, Hong Kong, China.

Received
31 July 2014Accepted
3 October 2014Published
23 October 2014Correspondence and
requests for materials
should be addressed to
J.G. (jugao@hku.hk)

Traditionally, strain effect was mainly considered in the materials with periodic lattice structure, and was thought to be very weak in amorphous semiconductors. Here, we investigate the effects of strain in films of cobalt-doped amorphous carbon (Co-C) grown on $0.7\text{PbMg}_{1/3}\text{Nb}_{2/3}\text{O}_3\text{-}0.3\text{PbTiO}_3$ (PMN-PT) substrates. The electric transport properties of the Co-C films were effectively modulated by the piezoelectric substrates. Moreover, we observed, for the first time, strain-induced photoconductivity in such an amorphous semiconductor. Without strain, no photoconductivity was observed. When subjected to strain, the Co-C films exhibited significant photoconductivity under illumination by a 532-nm monochromatic light. A strain-modified photoconductivity theory was developed to elucidate the possible mechanism of this remarkable phenomenon. The good agreement between the theoretical and experimental results indicates that strain-induced photoconductivity may derive from modulation of the band structure via the strain effect.

Amorphous carbon (a-C) films have attracted widespread attention for use in various device applications due to their remarkable electrical, magnetic and optical properties¹⁻⁶. The variability of these physical properties is directly correlated with the films' unique dual nanostructure in which sp^2 -hybridized nanoclusters are embedded in the sp^3 -hybridized matrix^{7,8}. Different deposition techniques and growing conditions can be used to control the sp^2/sp^3 ratio, and thus modulate the characteristics of a-C films^{8,9}. Another method, which is expected to induce interesting physical properties, is to form a more complicated structure that includes metallic nanoparticles surrounded by the a-C matrix. By choosing the type and size of these metallic nanoparticles, researchers can design a special a-C film with the desired magnetic and optoelectronic properties. Co and Ni have been found to form spontaneously as crystalline nanoparticles in a-C films, and considerable research effort has thus been devoted to the interplay between Co or Ni nanoparticles and their effect on various optoelectronic properties¹⁰⁻¹³.

The effects of strain have to date been investigated primarily in materials with a periodic lattice structure, and are thought to be very weak for amorphous materials¹⁴⁻¹⁷. However, the recent computational results demonstrated that the piezoresistive effect of a-C films could be strengthened by embedding crystalline nanoparticles into the carbon matrix¹³. Furthermore, the external strain might affect the optical gaps, and thus modulated their optoelectronic properties¹⁸. It is interesting to study the relationship between increased strain and the optoelectronic properties in a-C films. Until now the related experimental and theoretical research still remains lacking.

Here, thin films of cobalt-doped amorphous carbon (Co-C) were grown on $0.7\text{PbMg}_{1/3}\text{Nb}_{2/3}\text{O}_3\text{-}0.3\text{PbTiO}_3$ (PMN-PT) substrates. Co-doping was expected to enhance the films' sensitivity to strain. We then investigated the piezoresistive effect in these thin Co-C films. Piezoelectric PMN-PT substrates were used to strain the films reversibly, and strain was observed to induce photoconductivity. To explain such a remarkable phenomenon, a theoretic model has been developed. This basic model assumes that the band gap can be tuned via strain, thereby inducing photoconductivity from nothing. In addition to Co-C films, the model can be applied to other amorphous material systems.

The resistance of the Co-C film was measured using the four-probe method. The inset in Fig. 1a shows a schematic illustration of the electrical measurement. The bias electric field was applied across the Co-C/PMN-PT structure, and a resistor of 20 M Ω was connected in series with the PMN-PT substrate to protect the electrical meters in case there was a dielectric breakdown in the PMN-PT crystal. The leakage current was confirmed to be less than 10 nA under bias voltage of 500 V. Fig. 1a presents the hysteresis loop of resistance, with the electric field cycling from -500 V to +500 V. Here, we define $\Delta R/R = [R(V) - R(0)]/R(0)$, where $R(V)$ and $R(0)$ are the resistances of the Co-C film with and without the bias electric field, respectively. For the forward bias, the resistance increases as the positive voltage increases and reaches its maximum value (about 40%). For the reverse bias, it decreases with an increase in the negative voltage and reaches its minimum value (about -20%). This

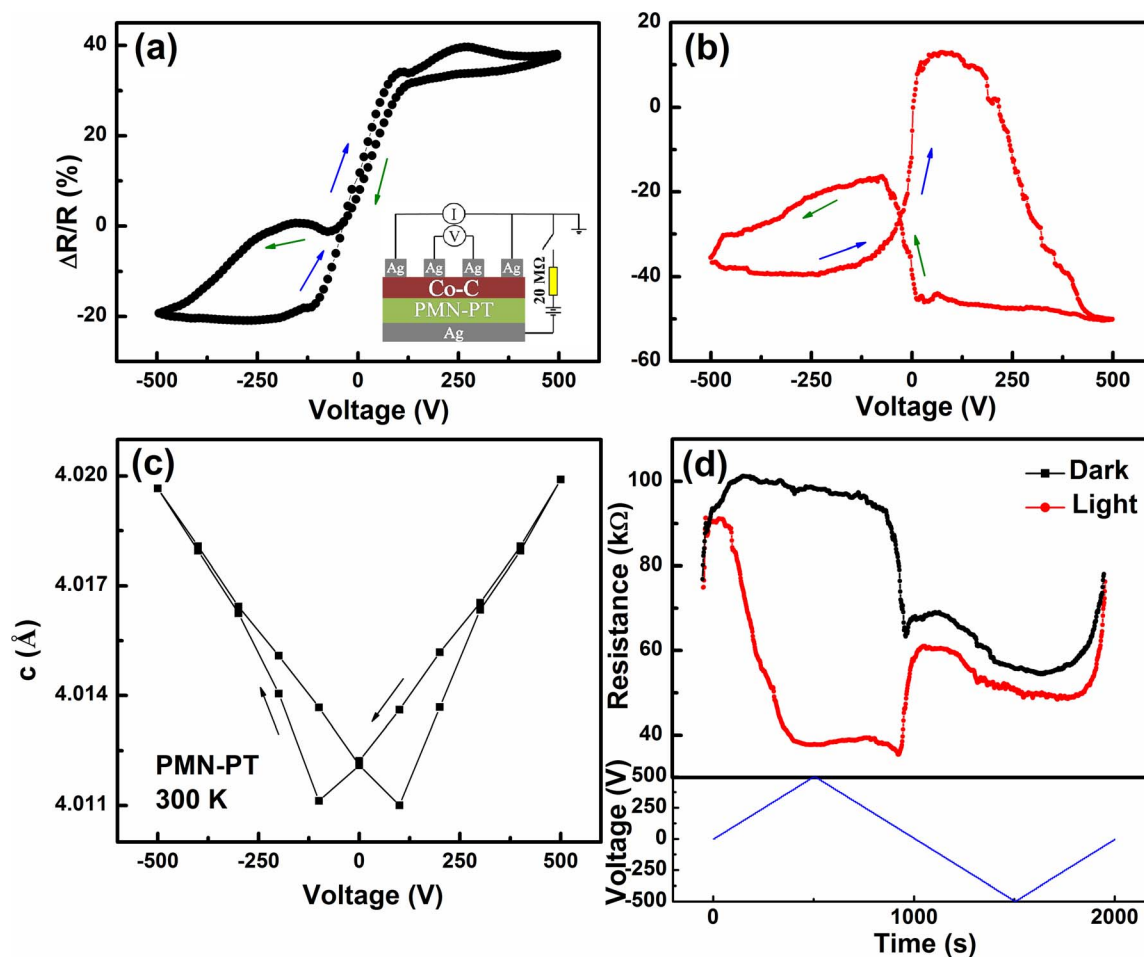


Figure 1 | The influence of strain in the electric properties. (a) Resistance hysteresis of the Co-C film versus the bias electric field at 300 K. The inset shows the schematic illustration of the electrical measurement. (b) Resistance hysteresis of the Co-C film as a function of the bias electric field under illumination of 50 mW/cm² at 300 K. (c) Out-of-plane lattice constant hysteresis of the PMN-PT substrate in the voltage range of [-500 V, 500 V]. (d) Resistance responses in a cycle of voltages (0 V \rightarrow 500 V \rightarrow -500 V \rightarrow 0 V) in darkness and under illumination.

phenomenon cannot be explained by the strain effect alone. The shuttle-like loop of the relative change in resistance indicates that the polarization effect is dominant in resistance modulation¹⁴. Major carriers in Co-C film are known to be holes. When a positive electric field is applied to a PMN-PT substrate ($V > 0$), the electric-dipole moments will point upward into the Co-C film. The accumulation of localized negative charges in the interface between the Co-C film and the PMN-PT substrate may trap free holes in the film, thereby causing the depletion of free holes and, in turn, increasing the resistance. In the case of applying a negative electric field ($V < 0$), the reverse effect may occur, with a decrease in resistance.

It is interesting to note that under illumination of 50 mW/cm² resistance hysteresis of the Co-C film changes from a shuttle-like loop to the butterfly-like loop shown in Fig. 1b, which implies that the strain effect rather than the polarization effect plays a dominant role in modulating the resistance. A possible explanation is as follows. In darkness, the number of localized electric charges in the interface between the Co-C film and PMN-PT substrate is comparable to that of the free holes in the Co-C film. Thus, the accumulation of localized electric charges in the interface has a great effect on the film's resistance. In contrast, under illumination, the incident light increases the free carriers largely by generating electron-hole pairs, which means that the number of carriers, trapped by the localized electric charges in the interface, is insufficient to influence the overall resistance of the sample. The influence of the polarization effect may be reduced by the incident light, with the strain effect becoming responsible for resistance hysteresis.

XRD measurements were used to investigate the response of the out-of-plane lattice constant c of PMN-PT (001) crystal under the applied electric field. In Fig. 1c, c exhibits a hysteresis behavior in a cycle of bias voltages. Considering that the stress tends to be transferred from the PMN-PT substrate to the Co-C film, observed resistance hysteresis may derive from ferroelectric hysteresis of the PMN-PT substrate. In addition, it is found that resistance hysteresis under illumination is more pronounced than that in darkness. In order to explain this phenomenon, the sample's conductivity can be expressed as $\sigma = \sigma_{\text{dark}} + \Delta\sigma_{\text{light}}$, where σ_{dark} is conductivity in darkness and $\Delta\sigma_{\text{light}}$ is conductivity increase induced by the incident light. σ_{dark} depends mainly on the charge polarization on the surface of the PMN-PT substrate, whereas $\Delta\sigma_{\text{light}}$ is a function of strain. In darkness, with $\sigma = \sigma_{\text{dark}}$, resistance hysteresis of the sample may be attributed only to hysteresis of the charge polarization. Under illumination, with $\sigma = \sigma_{\text{dark}} + \Delta\sigma_{\text{light}}$, the observed resistance is determined by the coaction of polarization and strain effects. The resistance hysteresis may be due to the sum of polarization and strain hystereses, thus being more pronounced than that in darkness.

Fig. 1d illustrates the resistance responses in a cycle of bias voltages with and without illumination. It should be pointed out that no significant photoconductivity was observed when the bias voltage was close to zero. It is thought that in this case, the Co-C film is no longer subject to the influence of the strain effect. This result is consistent with our previous observation that a-C films are insensitive to light because of their disordered structure. However, when the bias voltage is increased, a large degree of photoconductivity can

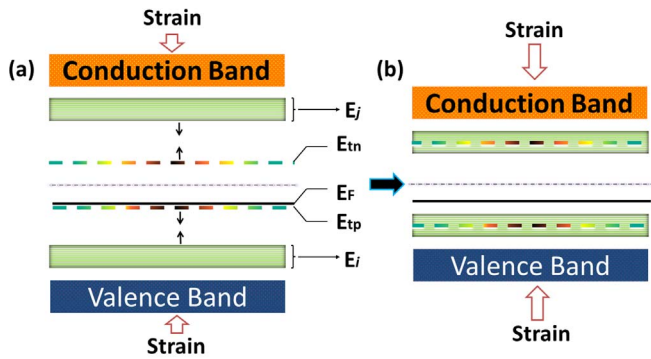


Figure 2 | Energy diagram of the Co-C film. The basic trap models of (a) weak strain and (b) strong strain.

be observed. At a bias voltage of 500 V, the resistance in darkness is almost three times larger than that under illumination. It seems that strain induces photoconductivity from nothing. Based on the strain effect, we constructed a modified model of photoconductivity in amorphous semiconductors to explain this remarkable phenomenon. Our model shows that the increase in strain can compress the band gap and thus enhance the photoconductivity effect.

Amorphous semiconductors are known to have a lattice structure with long-range disorder⁷. It is impossible to study their transport properties on the basis of such a disordered lattice structure. An alternative means of doing so is to make use of the Fermi-Dirac distribution function in these semiconductors. The band structure of amorphous semiconductors was elucidated by Mott *et al.*, as shown in Fig. 2¹⁹. The conduction or valence band has a tail of limited depth owing to the long-range disorder. M and N discrete π states are distributed at E_j and E_p , respectively, which are thought to depend on the medium-range order^{7,20}. In the case of Co-C films, these states may be influenced primarily by Co-doping.

Based on the band structure of amorphous semiconductors, Simmons and Taylor developed a theory of photoconductivity containing discrete trap levels²¹. To simplify the problem, the basic model contains two trap levels: one in the upper half of the band gap (E_{tn}) and the other in the lower half (E_{tp}), as shown in Fig. 2a. In accordance with the Co-C film being of p-type, the Fermi level (E_F) is situated in the lower half. E_{tp} is initially localized near the Fermi level, and E_{tn} near the reflected position of E_F with respect to the center of the band gap.

The generation rate of the electron-hole pairs can be written as²¹

$$G = \frac{np}{n+p} \rho_t \chi v \left\{ \sum_{i=1}^N \frac{1}{1 + \exp\left[\frac{E_{tp} - E_i}{kT}\right]} + \sum_{j=1}^M \frac{1}{1 + \exp\left[\frac{E_j - E_{tn}}{kT}\right]} \right\}, \quad (1)$$

where n and p are the concentrations of the free electrons and holes, respectively, ρ_t is the concentration of the trap levels, χ is the capture cross-sections of the electrons or holes for the trap, v is the thermal velocity and k is the Boltzmann constant. Under steady-state conditions, G is mainly dependent on the difference between E_{tp} (or E_{tn}) and E_i (or E_j). However, equation (1) cannot be used to analyze the strain-induced photoconductivity of Co-C films because of its irrelevance to the strain term. To solve this problem, we assume that the band gap decreases as a function of increasing strain. During this process, the compressed band gap may cause E_{tp} (or E_{tn}) and E_i (or E_j) to shift toward each other as shown in Fig. 2. The net effect is that the difference between E_{tp} (or E_{tn}) and E_i (or E_j) decreases as strain increases. Therefore, the strain term may be considered as

$$E_{tp}(s) - E_i(s) = \Delta E_i - \gamma_p s, \quad E_j(s) - E_{tn}(s) = \Delta E_j - \gamma_n s, \quad (2)$$

where ΔE_i and ΔE_j are determined by $E_{tp}(0) - E_i(0)$ and $E_j(0) - E_{tn}(0)$, respectively, γ_p and γ_n are named as strain-modified sensi-

vities depending on the material characteristics and s is the strain coefficient. Here, to simplify the problem we assume that $E_{tp}(s) - E_i(s)$ and $E_j(s) - E_{tn}(s)$ are both linear with s . Our simulation results showed this assumption to be reasonable in Co-C film. In other amorphous semiconductor systems, the relation between $E_{tp}(s) - E_i(s)$ [or $E_j(s) - E_{tn}(s)$] and s can always be calculated from experimental data. From equations (1) and (2), the strain-modified equation for the generation rate G of electron-hole pairs may be written as

$$G = \frac{np}{n+p} \rho_t \chi v \left\{ \sum_{i=1}^N \frac{1}{1 + \exp\left[\frac{\Delta E_i - \gamma_p s}{kT}\right]} + \sum_{j=1}^M \frac{1}{1 + \exp\left[\frac{\Delta E_j - \gamma_n s}{kT}\right]} \right\}, \quad (3)$$

Equation (3) allows us to build a bridge connecting rate G and strain s .

Photocurrent J_{ph} is normally defined as

$$J_{ph} = q \mathcal{E} (\mu_n \Delta n + \mu_p \Delta p), \quad (4)$$

where \mathcal{E} is the electric field, q is the charge of an electron, μ_n and μ_p are the mobility of electrons and holes, respectively. For a p-type semiconductor ($p \gg n$), J_{ph} is mainly dependent on Δp . Hence, $J_{ph} \cong q \mathcal{E} \mu_p \Delta p$.

In accordance with the photoconductivity theory of amorphous semiconductors, Δp_i at room temperature can be written as²¹

$$\Delta p_i = \frac{G}{v \chi \rho_t} \exp\left\{\frac{[\phi - (E_i - E_v)]}{kT}\right\}, \quad (5)$$

where ϕ is the activation energy and E_v the valence band. This equation, together with (3) and (4), describes the strain-induced photoconductive process in its entirety.

Now that we have a strain-modified photoconductivity theory of Co-C films, we look into their characteristics in more detail by examining two distinct ranges: weak strain and strong strain. In the case of weak strain ($s \approx 0$), as shown in Fig. 2a, equation (3) reduces to

$$G = \frac{np}{n+p} \rho_t \chi v \exp\left(\frac{\gamma_0 s}{kT}\right) \left[\sum_{i=1}^N \exp\left(\frac{-\Delta E_i}{kT}\right) + \sum_{j=1}^M \exp\left(\frac{-\Delta E_j}{kT}\right) \right], \quad (6)$$

where we assume $\gamma_p = \gamma_n = \gamma_0$. From equations (4), (5) and (6), we have

$$J_{ph}(s) = J_0 \exp\left(\frac{\gamma_0 s}{kT}\right). \quad (7)$$

Equation (7) shows that J_{ph} increases exponentially with weak strain s in Co-C films. Further, for amorphous semiconductors with a small value of γ_0 , the equation implies that J_{ph} may be linear with strain s .

In the case of strong strain (see Fig. 2b), the trap levels may penetrate E_i and E_j , thereby causing $\exp\left[\frac{\Delta E_i - \gamma_0 s}{kT}\right]$ and $\exp\left[\frac{\Delta E_j - \gamma_0 s}{kT}\right] \ll 1$. Similar to the calculation process for weak strain, we have

$$J_{ph}(s) = J_{\max} [1 - \alpha \exp(-\frac{\gamma_0 s}{kT})], \quad (8)$$

where α can be a constant determined by experimental results or by equations (3), (4) and (5). Equation (8) exhibits the saturation behavior of the photocurrent of Co-C films under strong strain. It is worth noting that maximum photocurrent J_{\max} depends on the number of discrete states at E_i and E_j rather than γ_0 .

Fig. 3a shows that the out-of-plane compressive strain [defined as $s_{\text{out}} = \frac{c(V) - c(V=0)}{c(V=0)}$] increases linearly with the bias voltage. In fact, out-of-plane expansion would be accompanied by contraction in both in-plane directions of PMN-PT single crystal. With the out-

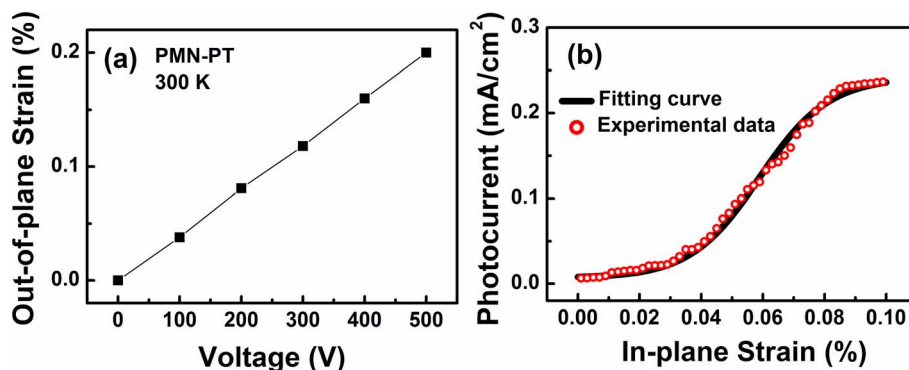


Figure 3 | Strain dependence of photocurrent. (a) Out-of-plane strain of the PMN-PT crystal under the electric bias field along the *c* axis at 300 K. (b) Photocurrent as a function of in-plane strain at 300 K. The red and open dots are obtained from measurements, and the black curve is the simulation using the strain-modified photoconductivity model.

of-plane strain equal to 0.2%, the in-plane tensile strain (s_{in}) was calculated as -0.1% by Poisson relation $s_{in} = -\frac{2u}{1-u}s_{out}$ using Poisson ratio $u = 0.2^{14,22}$. The in-plane tensile strain in the PMN-PT substrate can be transferred to the Co-C film. Thus, the absolute value of s_{in} is an appropriate substitute for the strain in the Co-C film. Fig. 3b illustrates the theoretical and experimental photocurrent as a function of s_{in} in Co-C films. To reduce the influence of relaxation effect in the PMN-PT substrate, we investigated photoconductivity with the bias voltage slowly increased from 0 to 500 V. Strain-modified sensitivity γ_0 is calculated as 117.3 eV from the experimental data. The fit parameters used to generate the fit curve in Fig. 3b were: $J_0 = 7.6 \times 10^{-3}$ mA/cm², $J_{max} = 0.247$ mA/cm², $\alpha = 7.06$. The theoretical simulation is highly consistent with the experimental data. In the strain range of $0 \sim 0.04\%$, the photocurrent exhibits an exponential increase with strain, whereas saturation behavior is observed in the strain range of $0.08 \sim 0.1\%$. Both phenomena are predicted by the proposed strain-modified photoconductivity theory.

In comparison with pure a-C films, Co-C films exhibit significant strain-modified photoconductivity. The discrete states at E_i and E_j are known to originate primarily from defects. Co-doping may influence the medium-range order in Co-C films, thus favoring the generation of these discrete states²⁰. The relation $J_{max} \sim M + N$ also means that the maximum photocurrent is enhanced by Co-doping. The model is not confined to the Co-C film system. The shapes of the photocurrent-strain characteristics are dependent on the magnitude of strain sensitivity γ_0 , as determined by amorphous materials. In some systems with a small γ_0 , no saturation behavior may be observed. In addition, strain-modified sensitivities γ_p and γ_n are not necessarily constants. They may be tuned by temperature or even by strain itself. In this case, $\gamma_p(T,s)$ and $\gamma_n(T,s)$ can be used to replace γ_0 when describing photoconductivity sensitivity to strain.

In summary, thin Co-C films were grown on PMN-PT substrates, and the effects of strain were investigated by applying electric fields to piezoelectric PMN-PT. Under illumination, a significant degree of photoconductivity was observed with an increase in strain. A strain-modified photoconductivity theory was then developed to elucidate the possible mechanism of this remarkable phenomenon. The basic model shows that the band gap can be tuned by strain, thus inducing photoconductivity from nothing. The photocurrent simulated using the model shows strong consistency with the experimental data. In addition to Co-C films, the theory proposed herein may also be applied to other amorphous material systems.

Methods

Samples preparation. Co-doped and undoped a-C films were grown on substrates of (001) oriented PMN-PT using the pulsed laser deposition method. Before deposition, the PMN-PT substrates were ultrasonically cleaned in ethanol, and then acetone, and

finally rinsed in deionized water. The deposition chamber was pumped to 6×10^{-6} mbar, and the substrates were heated to 400°C. A graphite disk with >99.99% purity embedded with a strip of cobalt (99.9%) was used as the target. Deposition was performed using a KrF excimer laser with 320 mJ/pulse energy and a frequency of 5 Hz for 10 min.

Microstructure observation. A scanning electron microscope (JEOL JSM-7001F, Japan) was used to observe the surface morphology and thickness (20 nm) of the samples. The Co concentration was analyzed via energy-dispersive X-ray spectroscopy, and found to reach 10%. Transmission electron microscopy (TEM) was performed using an FEI Tecnai G2 20 scanning TEM at 200 kV, and X-ray diffraction (XRD) was used to investigate the lattice displacement of the PMN-PT substrate with the application of external strain. Raman spectroscopy with a 514-nm laser (WITec-Alpha, Germany) was used to identify the disordered structures and measure the sp^2/sp^3 ratio, with Raman spectra acquired in the range of 1000 ~ 1800 cm⁻¹.

Electric measurement. Silver surface electrodes were evaporated on the Co-C films to ensure an ohmic contact. The resistance, current-voltage (I-V) relations and photoconductivity of the Co-C films were measured using the standard four-probe method with a Keithley 2400 SourceMeter. Monochromatic light illumination was provided by a semiconductor laser (wavelength $\lambda = 532$ nm) with variable power density, and the DC voltage across the PMN-PT was supplied by a Keithley 6487 voltage source. To limit the possibility of substrate crack as a result of polarization reversal, most measurements were carried out in a moderate range of [-500 V, 500 V].

1. Fyta, M. G., Remediakis, I. N., Keliros, P. C. & Papaconstantopoulos, D. A. Insights into the Fracture Mechanisms and Strength of Amorphous and Nanocomposite Carbon. *Phys. Rev. Lett.* **96**, 185503 (2006).
2. Lau, D. W. M. *et al.* Abrupt Stress Induced Transformation in Amorphous Carbon Films with a Highly Conductive Transition Phase. *Phys. Rev. Lett.* **100**, 176101 (2008).
3. Xue, Q. Z. & Zhang, X. Anomalous electrical transport properties of amorphous carbon films on Si substrates. *Carbon* **43**, 760–764 (2005).
4. Han, J. *et al.* Photovoltaic characteristics of amorphous silicon solar cells using boron doped tetrahedral amorphous carbon films as p-type window materials. *Appl. Phys. Lett.* **90**, 083508 (2007).
5. Wan, C., Zhang, X. Z., Zhang, X., Gao, X. L. & Tan, X. Y. Photoconductivity of iron doped amorphous carbon films on n-type silicon substrates. *Appl. Phys. Lett.* **95**, 022105 (2009).
6. Hsu, H. S. *et al.* Observation of bias-dependent low field positive magneto-resistance in Co-doped amorphous carbon films. *Appl. Phys. Lett.* **97**, 032503 (2010).
7. Robertson, J. Diamond-like amorphous carbon. *J. Mater. Sci. Eng. R.* **37**, 129–281 (2002).
8. Davis, C. A., Amarantunga, G. A. J. & Knowles, K. M. Growth Mechanism and Cross-Sectional Structure of Tetrahedral Amorphous Carbon Thin Films. *Phys. Rev. Lett.* **80**, 3280–3283 (1998).
9. Ferrari, A. C. & Robertson, J. Interpretation of Raman spectra of disordered and amorphous carbon. *Phys. Rev. B* **61**, 14095–14107 (2000).
10. Sato, K. *et al.* Direct imaging of atomic clusters in an amorphous matrix: A Co-C granular thin film. *Appl. Phys. Lett.* **101**, 191902 (2012).
11. Anton, R. In situ Transmission Electron Microscopy Study of the growth of Ni Nanoparticles on Amorphous Carbon and of the Graphitization of the Support in the Presence of Hydrogen. *J. Mater. Res.* **20**, 1837–1843 (2005).
12. Zhang, J. & Lan, C. Q. Nickel and cobalt nanoparticles produced by laser ablation of solids in organic solution. *Mater. Lett.* **62**, 1521–1524 (2008).



13. Koppert, R. *et al.* Structural and physical properties of highly piezoresistive nickel containing hydrogenated carbon thin films. *Diam. Relat. Mater.* **25**, 50–58 (2012).
14. Sheng, Z. G., Gao, J. & Sun, Y. P. Coaction of electric field induced strain and polarization effects in La_{0.7}Ca_{0.3}MnO₃/PMN-PT structures. *Phys. Rev. B* **79**, 174437 (2009).
15. Zheng, R., Wang, Y., Chan, H., Choy, C. & Luo, H. Determination of the strain dependence of resistance in La_{0.7}Sr_{0.3}MnO₃/PMN-PT using the converse piezoelectric effect. *Phys. Rev. B* **75**, 212102 (2007).
16. Hedler, A., Klaumunzer, S. L. & Wesch, W. Amorphous silicon exhibits a glass transition. *Nat. Mater.* **3**, 804–809 (2004).
17. Maiti, A. Carbon nanotubes: Bandgap engineering with strain. *Nat. Mater.* **2**, 440–442 (2003).
18. Mathioudakis, C. & Fyta, M. Disorder and optical gaps in strained dense amorphous carbon and diamond nanocomposites. *J. Phys. Condens. Matter.* **24**, 205502 (2012).
19. Mott, N. F., Davis, E. A. & Street, R. A. States in the gap and recombination in amorphous semiconductors. *Philos. Mag.* **32**, 961–996 (1975).
20. Robertson, J. Amorphous carbon. *Adv. Phys.* **35**, 317–374 (1986).
21. Simmons, J. G. & Taylor, G. W. Theory of photoconductivity in amorphous semiconductors containing relatively narrow trap bands. *J. Phys. C: Solid St. Phys.* **7**, 3051 (1974).
22. Thiele, C., Dörr, K., Bilani, O., Rödel, J. & Schultz, L. Influence of strain on magnetization and magnetoelectric effect in La_{0.7}A_{0.3}MnO₃/PMN-PT(001) (A = Sr, Ca). *Phys. Rev. B* **75**, 054408 (2007).

Acknowledgments

This work has been supported by the Research Grant Council of Hong Kong (Project code: 701813), the National Key Project for Basic Research (No. 2014CB921002) and the National Natural Science Foundation of China (Grant No. 11374225).

Author contributions

J.G. proposed and led the project. Y.C.J. conceived the idea, designed the experiments and developed the theory. Y.C.J. and J.G. wrote the manuscript and prepared all figures together.

Additional information

Competing financial interests: The authors declare no competing financial interests.

How to cite this article: Jiang, Y.C. & Gao, J. Strain-induced photoconductivity in thin films of Co doped amorphous carbon. *Sci. Rep.* **4**, 6738; DOI:10.1038/srep06738 (2014).



This work is licensed under a Creative Commons Attribution-NonCommercial-ShareAlike 4.0 International License. The images or other third party material in this article are included in the article's Creative Commons license, unless indicated otherwise in the credit line; if the material is not included under the Creative Commons license, users will need to obtain permission from the license holder in order to reproduce the material. To view a copy of this license, visit <http://creativecommons.org/licenses/by-nc-sa/4.0/>